On the Use of Excess Entropy Scaling to Describe the Dynamic Properties of Water

Ravi Chopra,[†] Thomas M. Truskett,[‡] and Jeffrey R. Errington*[,†]

Department of Chemical and Biological Engineering, University at Buffalo, The State University of New York, Buffalo, New York 14260, and Department of Chemical Engineering and Institute for Theoretical Chemistry, University of Texas at Austin, Austin, Texas 78712

Received: May 28, 2010; Revised Manuscript Received: June 24, 2010

We use molecular dynamics and transition-matrix Monte Carlo simulation to study the ability of entropy scaling relationships to describe kinetic properties of the extended simple point charge water model. We examine translational and rotational diffusivities, a characteristic relaxation time for rotational motion, and a collective relaxation time stemming from analysis of the coherent intermediate scattering function. We consider both the thermodynamic excess entropy and the contribution to the two-body excess entropy related to center-of-mass correlations as scaling variables. Calculations are performed over a broad range of conditions that span from the dense supercooled liquid regime to the critical region. We find that the thermodynamic excess entropy serves as a suitable metric for describing reduced transport properties for state conditions corresponding to temperatures above the onset of water's structurally anomalous region, defined by states points for which the excess entropy increases upon compression at constant temperature. In contrast, the aforementioned two-body contribution to the excess entropy cannot be used to quantitatively predict kinetic properties over the wide range of conditions explored here. For state points above the onset temperature of the structurally anomalous region, reduced transport property data collapse onto common curves when expressed as a function of the thermodynamic excess entropy. Below this temperature, data fall onto isochore-specific curves. Our results show a relatively strong correlation between the translational diffusivity and excess entropy and a noticeably weaker correlation between rotational mobility and excess entropy.

I. Introduction

Transport phenomena play an important role in a broad range of natural systems and engineered devices. Examples include the movement of biological molecules through complex intercellular environments, the flow of fluids in microfluidic devices, and the transport of light gases in nanostructured storage materials (e.g., metal−organic frameworks).[1] Quantitative modeling of these systems is completed with the assistance of kinetic properties, such as diffusivities, viscosities, thermal conductivities, and various relaxation times. It follows that the optimization of existing devices and development of new technologies benefit from a means to acquire these properties. In recent years, entropy scaling concepts[2−6] have reemerged as a tool for predicting the transport properties of a system through quasi-universal corresponding state relationships between kinetic parameters and the excess entropy. In this work, we use molecular simulation to examine the ability of these relationships to describe the dynamic properties of a common water model.

Excess entropy-scaling techniques utilize empirical relationships between thermodynamic and transport properties that enable prediction of one from the other.[5] In many cases, one is interested in using these relations to estimate difficult-to-predict transport properties from thermodynamic information alone.[7] Entropy-scaling ideas were first introduced in the late 1970s by Rosenfeld.[2,3] Within his framework, it is stipulated that transport coefficients (e.g., diffusivities, viscosities, and thermal conductivities) of dense fluids, nondimensionalized by appropriate combinations of macroscopic thermodynamic properties (e.g., temperature, density), approximately scale with the exponential of the excess entropy. In a series of seminal papers,[2−4] Rosenfeld and co-workers verified that the reduced diffusivities, viscosities, and thermal conductivities of simple model fluids (with a variety of different isotropic pair interactions) correlate well with the excess entropy over a wide range of thermodynamic conditions. Upon the basis of this work, Rosenfeld introduced quasi-universal "corresponding-states" relationships[5] that serve as a means to semiquantitatively predict a given transport property via knowledge of the excess entropy. Dzugutov later introduced an alternative scaling formalism for predicting the diffusion coefficient,[6] which also requires knowledge of microscopic structural information. To our knowledge, Dzugutov's scaling approach has not been generalized to predict other transport coefficients. Finally, in a collection of recent papers,[8−14] it has been shown that similar strategies can be used to describe the influence of confinement upon the transport properties of a fluid. Specifically, one finds that simple model fluids of particles with spherically symmetric pair potentials (e.g., atomistic fluids) confined within simple geometries (e.g., slit-pore, cylinder, square channel) under equilibrium conditions approximately exhibit the same relationship between self-diffusivity and excess entropy as the bulk fluid at a given temperature.

The application of entropy scalings for the transport coefficients of fluids consisting of particles with orientation-dependent pair potentials and intramolecular degrees of freedom (e.g., molecular fluids) has gathered attention only relatively recently. Given that many fluids of industrial relevance are molecular in nature, examination of entropy scaling ideas within the context of these fluids is clearly of interest. In the simplified case of an atomistic fluid, the excess entropy has a straightfor-

* Corresponding author. E-mail: jerring@buffalo.edu.
[†] University at Buffalo, The State University of New York.
[‡] University of Texas at Austin.

10.1021/jp1049155
Published on Web 07/23/2010

ward interpretation. It quantifies the reduction in the number of states (relative to an ideal gas) accessible to a system due to translational interparticle correlations, which arise from strong couplings between center-of-mass positions of neighboring particles in a liquid. These translational correlations between particles are important for interparticle collisions and act to reduce a single particle's ability to perform translational motion relative to its neighbors. Thus, it is intuitive that thermodynamic conditions which make the excess entropy of a dense fluid more negative also reduce translational self-diffusivity, increase shear viscosity, etc. In the case of molecular systems, translational, rotational, and intramolecular degrees of freedom all contribute to the excess entropy. For rigid molecules, one can formally decompose the excess entropy into a translational contribution related to center-of-mass positional correlations and an orientational term associated with correlations between the orientations of neighboring molecules.[15] Thus, it is natural to question whether the transport property of a molecular fluid associated with a particular type of motion scales with the component of the excess entropy related to the intermolecular correlations associated with those degrees of freedom or with the total (thermodynamic) excess entropy (or perhaps with neither). For example, does the translational self-diffusivity of molecular fluids scale with the component of the excess entropy related to center-of-mass positional correlations, to the total excess entropy, or to something else? Questions related to the use of scaling concepts for confined molecular fluids also require attention. Does confinement place unique constraints on molecular fluids that diminish the applicability of entropy scaling? Finally, molecular fluids highlight transferability issues related to entropy scaling relationships. To what extent can the scaling relationship for a given fluid (say argon) be applied to a fluid with a different architecture (say *n*-octane)?

Recent studies provide some insight into these questions. Initial work focused on accessing the ability of the two-body approximation to the translational component of the excess entropy to capture dynamic behavior. Mittal et al. found that the raw (not reduced) diffusivity of the extended simple point charge (SPC/E) model for water along a given isochore scaled approximately linearly with the two-body translational excess entropy over the temperature range 220−300 K.[16] The density dependence of the curves, however, was particularly noticeable, and no attempt was made to reduce the diffusion coefficient data via the Rosenfeld or Dzugutov approach. Johnson and Head-Gordon later performed a similar analysis with the TIP4P-Ew water model.[17] They found that the linear nature of the aforementioned scaling broke down at very low temperatures. They also observed that reducing the diffusion coefficients via the Dzugutov approach[6] did not alter the quality of the scaling.

Experimental studies by Abramson and co-workers have provided insight regarding the ability of the total (thermodynamic) excess entropy to serve as a useful descriptor of transport properties. Abramson measured the shear viscosity of water over a range of conditions spanning from ambient up to 300 °C and 6 GPa and examined the ability of Rosenfeld scaling to describe the data.[18] He found that reduced viscosity data from all state points approximately collapse onto a common curve when expressed as a function of the thermodynamic excess entropy. However, the composite curve was decidedly nonlinear, in contrast to what has been observed for atomistic fluids. Moreover, the common curve was significantly removed from the "universal" corresponding-states relation introduced by Rosenfeld for atomistic fluids. In a subsequent study,[19] Abramson and West-Foyle focused on small linear molecules, including nitrogen, oxygen, and carbon dioxide. Again, they demonstrated that reduced viscosity data collapse onto species-specific common curves when plotted versus the thermodynamic excess entropy. In this latter case, the composite curves were found to be relatively linear.

Goel et al. studied transport-thermodynamic property relationships for Lennard-Jones chains.[20] They employed molecular dynamics simulation to calculate self-diffusivity and viscosity values and approximated the total excess entropy using both the self-associating fluid theory (SAFT)[21,22] and a two-body simplification related to monomer−monomer pair correlations. Both reduced diffusivities and viscosities were found to scale approximately linearly with the exponential of the excess entropy. Similar to the Abramson and West-Foyle study,[19] data were found to collapse onto species-specific curves. This observation was also reported by Gerek and Elliott,[23] who used discontinuous molecular dynamics simulation and thermodynamic perturbation theory to examine the robustness of Rosenfeld scaling relations for the *n*-alkane homologous series. Most recently, Agarwal and co-workers have used molecular simulation to probe the effectiveness of Rosenfeld scaling for common water models[24] and network forming ionic melts.[24−26] In the case of water, they find that reduced self-diffusivity data collapse onto weakly isochore-dependent curves when expressed as a function of the thermodynamic excess entropy. In contrast, they report that the two-body approximation to the translational component of the excess entropy does not serve as an effective scaling parameter.

Collectively, the studies outlined above suggest that excess entropy scaling concepts can be, at least in some cases, used to successfully describe the transport properties of molecular fluids. For the cases tested thus far, the total excess entropy has proven to be the most reliable scaling variable. One also, however, finds that the "universal" exponential scaling function introduced by Rosenfeld[5] does not extend beyond atomistic fluids. Instead, a unique scaling relationship exists for each molecular species. Water appears to distinguish itself from the other fluids tested in that standard scaling relations exhibit a high degree of curvature or show isochore dependence, which has only otherwise been found in the deeply supercooled fluid state of atomic fluids.[27]

In this work, we further investigate entropy scaling concepts for water. Specifically, we examine the translational self-diffusion coefficient of the SPC/E water model[28] over a somewhat broader range of conditions than probed by Agarwal and co-workers.[24] Importantly, we also study three additional dynamic quantities: the rotational diffusion coefficient, a relaxation time for rotational motion, and a collective relaxation time. Given the known breakdown[29,30] of the Stokes−Einstein[31] and Stokes−Einstein−Debye[32] relations, along with the related decoupling of translational and rotational mobility, observed with common water models, one might expect to find varying levels of success in using the excess entropy to describe dynamic properties.

We find that the Rosenfeld reduced translational diffusivity and collective relaxation time data each approximately collapse to single curves when plotted against the thermodynamic excess entropy for all densities studied at temperatures above water's structurally anomalous region, defined as the collection of state points for which the thermodynamic excess entropy increases upon isothermal compression. The two measures of rotational mobility also approximately collapse onto single curves, but the quality of the correlation is poor relative to the aforemen-

tioned dynamic properties. Within the structurally anomalous region, all transport properties fall onto isochore-specific curves.

The paper is organized as follows. In the following section, we describe the model examined in this work and the molecular simulation methods used to compute thermodynamic and transport properties of interest. Next, we present our simulation results for the evolution of the dynamic properties with temperature and density and discuss the ability of Rosenfeld scaling to capture the trends observed.

II. Molecular Simulations

Molecular Model. We work with the extended simple point charge (SPC/E) model for water.[28] This fixed point charge model consists of a Lennard-Jones center located on the oxygen atom and point charges placed at the centers of the oxygen and two hydrogen atoms. The OH distance is 1.0 Å, and the HOH angle is 109.47°. The Lennard-Jones interaction is characterized by size and energy parameters of $\sigma = 3.166$ Å and $\varepsilon = 0.6502$ kJ/mol, respectively. Charges on the hydrogen and oxygen atoms equal 0.4238e and −0.8476e, respectively, where e is the fundamental unit of charge.

Structural Properties. In this work, we consider two versions of the excess entropy. The first is the total thermodynamic excess entropy s^{ex}, which accounts for all intermolecular (two-, three-, and higher-body)[33−35] correlations, including translational contributions related to center-of-mass positional correlations and orientational contributions associated with correlations between the orientations of neighboring molecules.[15] In the section immediately below, we detail how this quantity is computed. In the second case, we aim to capture the translational contribution to the excess entropy only. Computing the contributions to the translational term related to three- and higher-body correlations is known to be a challenging task.[33−35] As a result, we restrict our attention to the two-body approximation to the translational component of the excess entropy $s_t^{(2)}$. We compute this quantity using information related to the structure of the fluid

$$s_t^{(2)}/k = -2\pi(\rho/M)\int \{g_{OO}(r)\ln[g_{OO}(r)] - [g_{OO}(r) - 1]\}r^2 dr \quad (1)$$

where k is Boltzmann's constant; ρ is the mass density; M is the molecular mass of water; and $g_{OO}(r)$ is the oxygen−oxygen pair correlation function. Calculating both s^{ex} and $s_t^{(2)}$ allows us to address one of the questions posed within the Introduction: does the translational self-diffusivity of molecular fluids scale with the component of the excess entropy related to center-of-mass positional correlations ($s_t^{(2)}$), the total excess entropy (s^{ex}), or something else? Ideally, we would also address the analogous question related to the connection between the rotational diffusivity and the orientational contribution to the excess entropy. However, calculation of just the two-body approximation to the orientational component of the excess entropy $s_o^{(2)}$ is a difficult task. Lazaridis and Karplus[15] first described the complex nature of this calculation, which requires collection and subsequent integration over a distance and orientation-dependent pair distribution function characterized by the center-of-mass separation distance and five independent angles that provide the mutual orientation of two molecules. Due to the demanding nature of this calculation, only a few "full" calculations of $s_o^{(2)}$ (for a very limited number of state points) have been completed with water models.[36−39] While several approximate strategies have been introduced,[15,40] relatively little is known regarding the accuracy of these approximate methods.[39] Given the computational demand of the full calculation of $s_o^{(2)}$ and the uncertainty in the accuracy of the approximate methods for computing $s_o^{(2)}$, we decided not to focus on this quantity here. Finally, we note that other approximate strategies for computing the total two-body contribution $s^{(2)} = s_t^{(2)} + s_o^{(2)}$ (for rigid molecules) to the excess entropy from atom−atom pair correlation functions have also been introduced.[41] Again, due to a lack of rigorously obtained data for the total two-body excess entropy, it is difficult at present to assess the accuracy of these approximate methods. The interested reader should refer to ref 24 for information related to the use of an approximate two-body excess entropy within the context of entropy-scaling strategies for water.

Thermodynamic Properties. We employ free-energy-based simulation techniques to evaluate the thermodynamic excess entropy. Here, excess properties are defined as the difference between the property of a real fluid and an ideal gas at the same temperature and density. In previous work,[7−11] excess entropy values along a specified isotherm were computed using grand canonical transition matrix Monte Carlo simulation (GC-TMMC).[42,43] For the model considered here, direct grand canonical simulation becomes difficult to implement at low temperatures and/or high densities. As a result, we employ a two-step process to determine the free energy at these conditions. In the first step we obtain the density dependence of the Helmholtz free energy at relatively high temperature (where sampling difficulties are not encountered) using GC-TMMC simulation. In the second step we perform a canonical temperature expanded ensemble (TE) simulation[44] to evaluate the change in Helmholtz free energy with temperature at constant density. Collectively, these simulations provide the excess Helmholtz free energy at a given temperature and density of interest. These simulations also enable us to determine the excess energy at a state point of interest via a straightforward ensemble average. The two aforementioned excess quantities are then combined via standard thermodynamic relationships to yield the excess entropy.

GC-TMMC simulations[42] are conducted at a specified temperature T, volume V, and activity $\xi = q\exp(\beta\mu)$, where $\beta = 1/kT$ is the inverse temperature; μ is the chemical potential; and q represents the component of the molecular partition function stemming from integration over momenta. The key quantities extracted from each simulation are the particle number (density) probability distribution $\Pi(N)$ and the particle-number-specific configurational energy $U(N)$. The intramolecular degrees of freedom are constrained within the model considered here, such that the ideal gas configurational energy is zero at all temperatures, and $U = U^{ex}$. The grand canonical particle number probability distribution provides the density dependence of the excess Helmholtz free energy $F^{ex}(N)$[7]

$$\beta F^{ex}(N) = -\ln[\Pi(N)/\Pi(0)] + N\ln\xi V - \ln N! \quad (2)$$

The excess entropy then follows from

$$S^{ex}/k = \beta U^{ex} - \beta F^{ex} \quad (3)$$

In practice, we prespecify the range of densities over which we wish to evaluate the Helmholtz free energy and employ multicanonical sampling techniques[45] within the GC-TMMC approach to encourage the simulation to visit low-probability states. Figure 1 provides data produced from a GC-TMMC simulation of SPC/E water at $T = 1000$ K, $\xi = 1$ Å^{-3}, and V

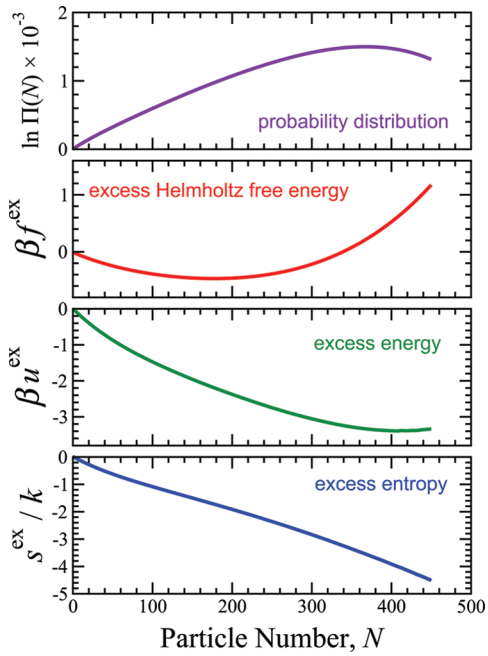

Figure 1. Illustration of the results obtained from GC-TMMC simulation of SPC/E water with $T = 1000$ K, $\xi = 1$ Å^{-3}, and $V = 10\,000$ Å^3.

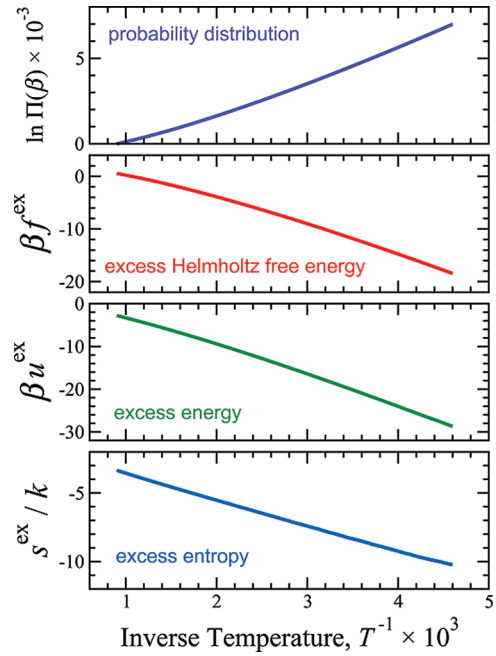

Figure 2. Illustration of the results obtained from TE-TMMC simulation of SPC/E water with $N = 368$ and $V = 10\,000$ Å^3.

$= 10\,000$ Å^3. Uncertainties in βf^{ex}, βu^{ex}, and s^{ex}/k are less than 8×10^{-4}, 7×10^{-3}, and 7×10^{-3}, respectively.

A canonical temperature expanded ensemble[44,46] consists of a collection of subensembles that share the same particle number and volume while possessing different temperatures. In this work, we take the inverse temperature β as the order parameter and establish a set of subensembles that range from β_{min} to β_{max} in increments of $\Delta\beta$. For convenience, we label the subensembles with integer values m that range from $m = 0$ to $m = M$. During a Monte Carlo simulation, the system attempts to transition between neighboring subensembles. The relative probabilities $\Pi(\beta_m)$ and $\Pi(\beta_q)$ of the system visiting subensembles m and q are directly related to the configurational partition function $Z(\beta)$

$$\frac{Z(\beta_m)}{Z(\beta_q)} = \frac{\Pi(\beta_m)}{\Pi(\beta_q)} \tag{4}$$

For the specific case examined here in which the ideal gas configurational energy is zero at all temperatures, the variation in the excess Helmholtz energy with temperature is obtained directly from the inverse temperature probability distribution

$$\beta_m F^{ex}(\beta_m) - \beta_q F^{ex}(\beta_q) = -\ln\left[\frac{\Pi(\beta_m)}{\Pi(\beta_q)}\right] \tag{5}$$

Therefore, provided one can measure the probability distribution $\Pi(\beta_m)$, TE simulation provides a means to evaluate the temperature dependence of F^{ex}.

In this work, we employ a transition matrix Monte Carlo (TMMC) algorithm[47,48] to estimate subensemble relative free energies. The approach is analogous to the GC-TMMC method described above as well as other expanded ensemble schemes that have been pursued.[12,46,49−51] To obtain an estimate of $\Pi(\beta_m)$, a standard canonical expanded ensemble simulation is performed with a simple bookkeeping scheme[48] that enables one to deduce the subensemble transition probabilities. These transition probabilities are subsequently used to compute the subensemble probabilities $\Pi(\beta_m)$. Figure 2 provides data produced from a TE-TMMC simulation of SPC/E water at $N = 368$ and $V = 10\,000$ Å^3 ($\rho = 1.101$ g/cm^3). Uncertainties in βf^{ex}, βu^{ex}, and s^{ex}/k are less than 1.5×10^{-3}, 2.7×10^{-2}, and 2.7×10^{-2}, respectively. As one might expect, the precision deteriorates with decreasing temperature as the system progressively moves through configuration space at a slower rate.

The free-energy approach pursued here has advantages over exponential averaging (e.g., single-stage free-energy perturbation)[52,53] and thermodynamic integration schemes.[54] While all of these methods provide accurate free-energy estimates when used appropriately, recent studies suggest that methods within the TMMC class have advantages from a rigor and efficiency standpoint. The transition matrix algorithm[47,48] is closely related[51,55] to Bennett's acceptance ratio method[56] and falls within a general class of two-sided free-energy methods that use information from both forward and reverse paths connecting two states of interest to compute a free-energy difference. Unlike thermodynamic integration schemes that rely upon discretization of the integration space and exponential averaging techniques, methods that fall within the Bennett class are known to be asymptotically unbiased, meaning that a free-energy estimate will approach the true (unbiased) value as the number of measurements becomes large.[57−59] Two-sided methods have also proven to be efficient.[57,59] Shirts and Pande recently compared the performance of exponential averaging, thermodynamic integration, and Bennett methods and found the Bennett scheme to be superior for realistic molecular systems.[59] Finally, we note that the free-energy approach pursued here is readily extendable to confined fluids.

Transport Properties. We calculate the translational self-diffusivity D_t by fitting the long-term behavior of the mean square displacement of oxygen atoms using the Einstein relation

$$\lim_{t\to\infty}\langle|\vec{r}(t') - \vec{r}(t)|^2\rangle = 6D_t t \tag{6}$$

where $\vec{r}(t')$ and $\vec{r}(t)$ are position vectors of an oxygen atom at times t' and t, respectively. We calculate a rotational diffusivity using an approach introduced by Kammerer et al.[60] and later adapted by Mazza et al.[29,61] to study water. Within this approach, one first selects a polarization vector. In this work, we limit ourselves to a single description, where the normalized polarization vector $\hat{p}_i(t)$ for molecule i is defined by the line extending from the center of mass of the water molecule to the midpoint of the line joining the two hydrogen atoms. Next, we define the vector rotational displacement as

$$\vec{\varphi}_i(\Delta t) = \int_t^{t+\Delta t} \Delta\vec{\varphi}_i(t')\mathrm{d}t' \tag{7}$$

where $\Delta\vec{\varphi}_i(t')$ is a vector with direction given by $\hat{p}_i(t') \times \hat{p}_i(t' + \mathrm{d}t')$ and with magnitude given by $|\Delta\vec{\varphi}_i(t')| = \cos^{-1}[\hat{p}_i(t')\hat{p}_i(t' + \mathrm{d}t')]$. We calculate the rotational diffusivity D_r by fitting the long-term behavior of the rotational mean square displacement

$$\lim_{t\to\infty}\langle|\vec{\varphi}_i(t') - \vec{\varphi}_i(t)|^2\rangle = 4D_r t \tag{8}$$

where $\vec{\varphi}_i(t')$ and $\vec{\varphi}_i(t)$ are vectors that define a trajectory in three-dimensional space representing the accumulated rotation of water molecule i at times t' and t, respectively.

To complement the translational and rotational diffusion coefficients, we also evaluate a collective relaxation time and dipole relaxation time. The collective relaxation time τ is defined as the time required for the normalized coherent intermediate-scattering function $F(q_0,t)$ to decay to a value of e^{-1}. The wavenumber q_0 corresponds to the approximate location of the first peak in the structure factor. The dipole relaxation time τ_2 associated with the rotational motion of a water molecule is defined by the time required for the correlation function $\langle P_2[\cos\theta(t)]\rangle$ to decay to a value of e^{-1}. P_2 is the second Legendre polynomial, and $\theta(t)$ is the angle defined by the orientations of the dipole moment vector of a molecule at times t and zero.

Simulation Details. We performed Monte Carlo (MC) and molecular-dynamics (MD) simulations to acquire thermodynamic and kinetic data over the range of state conditions defined by $220 < T < 500$ K and $0.85 < \rho < 1.30$ g/cm^3. For all simulations, we used a cell with volume $V = 10\,000$ Å^3. A single GC-TMMC simulation was completed at $T = 1000$ K with $\ln \xi = 0$. TE-TMMC simulations were completed over the inverse temperature range $T^{-1} = 0.9 \times 10^{-3}$ to 4.6×10^{-3} K^{-1}, with a subensemble spacing of $\Delta T^{-1} = 2.0 \times 10^{-6}$ K^{-1}. Within the molecular dynamics simulations, the temperature was controlled using a Nosé−Hoover thermostat,[62,63] and the system was propagated using the velocity-Verlet method[64,65] with a time step of 1 fs. More specifically, we employ a chain of five Nosé−Hoover thermostats,[66] with the "mass" of the first thermostat corresponding to a coupling constant of $\tau_{T_1} = 1.0$ ps, and the remaining four thermostats with $\tau_{T_{i\neq1}} = \tau_{T_1}/3N$. The influence of the coupling constant τ_T on the mean-squared displacement has been discussed by Frenkel and Smit.[54] The RATTLE algorithm[67] was used to maintain the geometry of the water molecule. In all cases, the Ewald summation method[54] was used to compute electrostatic energies and forces.

Statistical uncertainties were determined by performing four independent sets of simulations. The standard deviation of the results from the four simulation sets was taken as an estimate of the statistical uncertainty.

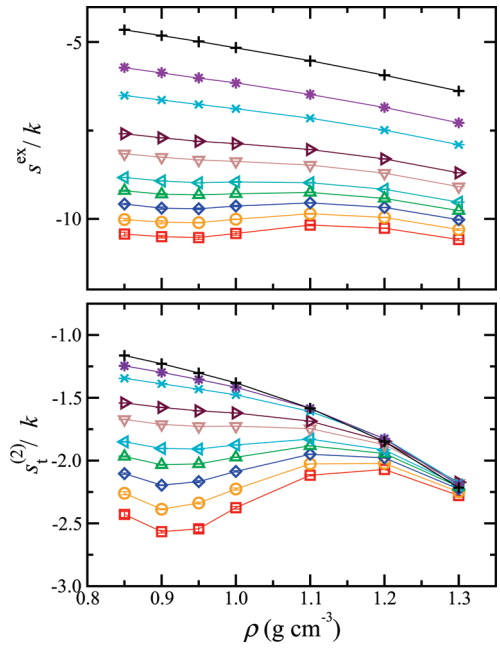

Figure 3. Evolution of the thermodynamic (top panel) and two-body (bottom panel) excess entropies with density along select isotherms. Curves from bottom to top are for $T = 220$, 230, 240, 250, 260, 280, 300, 350, 400, and 500 K.

III. Results and Discussion

Figure 3 provides the temperature and density dependence of the excess entropies s^{ex} and $s_t^{(2)}$. The excess entropy is often used as a measure of the fluid's structural order.[68] The region of state points within which a metric for structural order increases upon isothermal compression has been used to define a structurally anomalous region within previous studies.[69] It is inside of the structurally anomalous region that one also typically finds state points for which the fluid exhibits anomalous kinetic (e.g., diffusivity, viscosity) and thermodynamic (e.g., density, excess entropy) behavior.[7,69−72] We define the structurally anomalous region with respect to s^{ex} here. This selection leads to an onset temperature for the structurally anomalous region of $T \approx 270$ K. The analogous onset temperature based upon the pair translational structural metric $s_t^{(2)}$ is $T \approx 280$ K. For completeness, we note that Errington and Debenedetti[69] originally used another related translational order parameter introduced by Truskett et al.[68] to define this region. Adopting this order metric results in a qualitatively similar, yet quantitatively broader, region of state points that display structural anomalies, characterized by an onset temperature of $T \approx 320$ K.

The observation of density anomalies, wherein $(\partial\rho/\partial T)_P > 0$, has long been established for SPC/E water.[69,73] Standard thermodynamic relationships[7,74,75] indicate that density anomalies are consistent with entropy anomalies, for which $(\partial s/\partial\rho)_T > 0$. Upon the basis of the definition employed here for the excess entropy, it follows that density anomalies mandate the existence of a broader region of anomalous excess entropy behavior,[7] wherein $(\partial s^{ex}/\partial\rho)_T > 0$. Indeed, here we find a region of excess entropy anomalies below $T \approx 270$ K and a region of entropy (density) anomalies below $T \approx 245$ K.

A comparison of the magnitudes of $s_t^{(2)}$ and s^{ex} reveals that $s_t^{(2)}$ provides just a small fraction of the overall contribution to s^{ex}. Others have reported[15] that the magnitude of the orientational contribution to the two-body excess entropy $s_o^{(2)}$ is considerably larger than that due to translational correlations ($s_t^{(2)}$). Our calculations indicate that $s_t^{(2)}/s^{ex}$ varies between 20 and 35% for

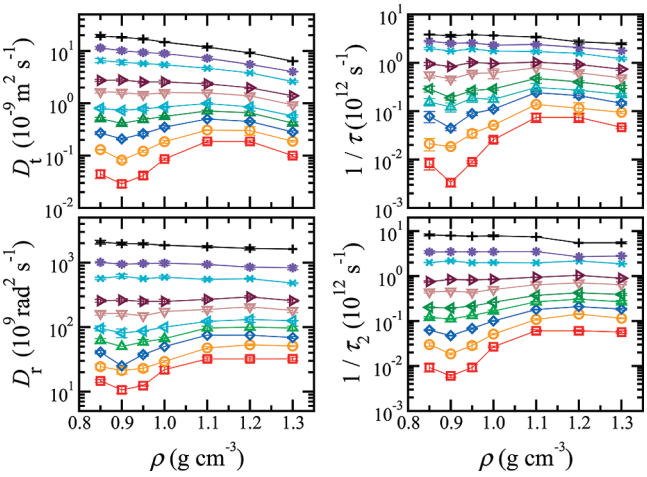

Figure 4. Evolution of the translational diffusion coefficient (top left panel), collective relaxation time (top right panel), rotational diffusion coefficient (bottom left panel), and rotational relaxation time (bottom right) with density along select isotherms. Curves from bottom to top are for T = 220, 230, 240, 250, 260, 280, 300, 350, 400, and 500 K.

the conditions examined here. Given the large difference in the magnitudes of the translational and orientational contributions to the two-body excess entropy, it is perhaps surprising that $s_t^{(2)}$ provides the level of insight that it does regarding water's anomalous behavior.[69] This notion is consistent with the level of success enjoyed by spherically symmetric core-softened models in qualitatively reproducing water's thermodynamic and transport behaviors.[7,76−78]

Figure 4 provides the temperature and density dependence of the kinetic properties D_t, D_r, τ, and τ_2. Our results are consistent with those reported in previous studies.[29,79] All of the dynamic properties display anomalous behavior at sufficiently low temperature. We find the onset of kinetic anomalies between T = 280 and 300 K. Errington et al. previously described[7] how Rosenfeld scaling ideas can be used to link regions of anomalous transport behavior to an analogous region of excess entropy anomalies. There it was suggested that an excess entropy anomaly "announces" the approach of transport anomalies, with the latter triggered when the strength of the excess entropy anomaly $(\partial s^{ex}/\partial\rho)_T$ reaches a property-specific value. This picture was based upon the universal scaling relations Rosenfeld introduced,[5] which are quantitatively accurate for atomistic fluids only. In this work, we again see a close connection between excess entropy and kinetic anomalies. Interestingly, for the SPC/E water model, we find that regions of anomalous transport behavior are broader than the corresponding region for the excess entropy. A similar result was obtained by Shell et al. in a study focused on silica.[70]

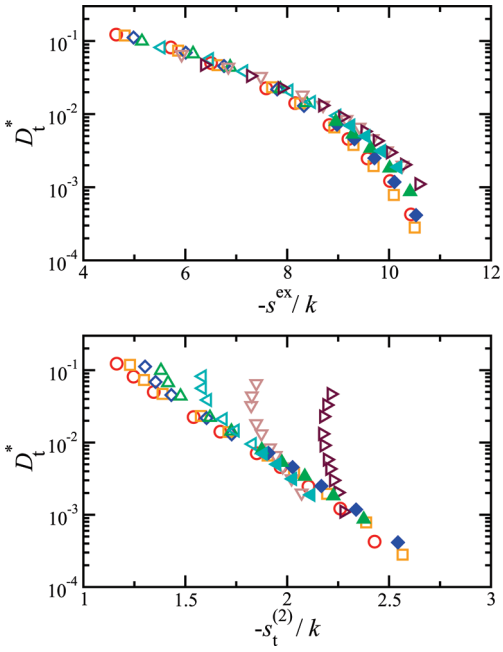

Figure 5. Relationship between reduced translational diffusivity and excess entropy. The top and bottom panels provide this relationship with the thermodynamic excess entropy and translational contribution to the two-body excess entropy, respectively. Circles, squares, diamonds, up triangles, left triangles, down triangles, and right triangles correspond to densities of ρ = 0.85, 0.90, 0.95, 1.00, 1.10, 1.20, and 1.30, respectively. State points within the structurally anomalous region, defined by $(\partial s^{ex}/\partial\rho)_T > 0$, are now denoted with filled symbols.

We now turn our attention toward the use of entropy scaling relations to describe the kinetic properties of water. We adopt a Rosenfeld-style approach[5] in which kinetic properties are reduced by macroscopic thermodynamic properties, such as temperature and density. More specifically, we work with the following quantities

$$D_t^* = D_t \frac{(\rho/M)^{1/3}}{(kT/M)^{1/2}} \tag{9}$$

$$D_r^* = D_r \frac{1}{(kT/M)^{1/2}(\rho/M)^{1/3}} \tag{10}$$

$$\frac{1}{\tau^*} = \frac{1}{\tau}\frac{1}{(kT/M)^{1/2}(\rho/M)^{1/3}} \tag{11}$$

$$\frac{1}{\tau_2^*} = \frac{1}{\tau_2}\frac{1}{(kT/M)^{1/2}(\rho/M)^{1/3}} \tag{12}$$

In what follows, we examine the extent to which $s_t^{(2)}$ and s^{ex} can be used to forecast a given reduced kinetic property.

Figure 5 shows the $D_t^*-s_t^{(2)}$ and $D_t^*-s^{ex}$ relationships for SPC/E water. It is clear that $s_t^{(2)}$ does not provide a suitable metric for collapsing diffusivity data over the wide range of conditions examined here. As was reported by Agarwal et al.,[24] each isochore forms a distinct curve within the $D_t^*-s_t^{(2)}$ space. In general, information related to center-of-mass positional correlations alone cannot be used to quantitatively describe the mobility of water molecules. In contrast, the thermodynamic excess entropy s^{ex} does provide a means to describe the diffusive behavior of water at sufficiently high temperature. More specifically, we find that all $D_t^*-s^{ex}$ points associated with temperatures above the onset of the structurally anomalous region defined by the excess entropy approximately collapse onto a common curve. Below this onset temperature, $D_t^*-s^{ex}$ points form isochore-specific curves. We find some evidence in Figure 5 that suggests that low-temperature points outside of the structurally anomalous regime collapse onto one of two common curves associated with the low- and high-density regions external to the anomalous region. However, a more extensive set of data for the low-temperature liquid will be

required to clarify the generality of this apparent bifurcation of the $D_t^*-s^{ex}$ curve.

We note that while we did not examine the relationship between D_t^* and the total two-body excess entropy $s^{(2)}$ here (for reasons discussed above), we suspect that D_t^* would correlate much stronger with $s^{(2)}$ than it does with $s_t^{(2)}$. In fact, based on the available simulation data, one might generally expect that the closer a potential scaling metric correlates with the total excess entropy s^{ex}, the more successful it will be in collapsing D_t^* data. As mentioned above, unfortunately, relatively little is currently known about $s^{(2)} = s_t^{(2)} + s_o^{(2)}$ for common water models due to the difficulty of accurately computing this quantity over a wide range of thermodynamic conditions. Nonetheless, within the recent study of Agarwal et al.[24] an approximate version of $s^{(2)}$, based upon atom−atom pair correlation functions, was examined and found to correlate stronger with D_t^* than the translational component $s_t^{(2)}$ did, which seems to be consistent with the aforementioned expectation. Finally, we note that the use of Dzugutov's approach to reduce the translational diffusion coefficient does not substantially change the picture presented here. Both Rosenfeld and Dzugutov scaling formalisms lead one to the same qualitative observations, and quantitative differences between the two are minor.

Rosenfeld suggested that $\ln(D_t^*)$ should approximately scale linearly with s^{ex} for condensed fluids.[5] The composite curve displayed in the top panel of Figure 5 clearly exhibits curvature. This observation is consistent with the experimental study of Abramson,[18] wherein it was found that Rosenfeld-reduced viscosity data collapse onto a common nonlinear curve when expressed as a function of the thermodynamic excess entropy. For atomistic fluids, one typically does not observe such curvature until relatively large values of $-s^{ex}$.[8,10,27] Here, we find curvature at nearly all values of $-s^{ex}$, with the degree of curvature increasing with increasing $-s^{ex}$. From a practical perspective, this diminishes the predictive ability of Rosenfeld scaling. Provided a linear relationship exists between $\ln(D_t^*)$ and s^{ex}, one simply needs to acquire D_t^* and s^{ex} at two state points to reliably predict diffusivity values at liquid conditions for which s^{ex} is known. When this linear relationship no longer holds, of course, one must acquire more initial data to make reasonable quantitative predictions.

The observation of a breakdown of Rosenfeld scaling within a region defined by anomalous excess entropy behavior is consistent with previous studies focused on core-softened fluids. For example, Krekelberg et al. recently considered the Gaussian-core model,[80−82] which exhibits anomalous behavior (with respect to the excess entropy) for state points with densities above a temperature-dependent value. Unlike liquid water, however, the Gaussian-core fluid never "recovers" normal (i.e., simple fluid) behavior at sufficiently high density because of the soft and bounded form of its interparticle interaction. For the Gaussian-core fluid, Rosenfeld scaling with the thermodynamic excess entropy fails to collapse diffusivity data within the anomalous region. Instead, as Krekelberg et al. first noted,[80] one finds distinct isochore-specific $D_t^*-s^{ex}$ curves that shift upward with increasing density. A similar breakdown of the Rosenfeld diffusivity scaling for fluids of Hertzian particles has since also been reported in a simulation study by Fomin et al.[83] As was discussed by Krekelberg et al.[80] and by Fomin et al.,[83] this breakdown is likely due to the fact that the Gaussian-core and Hertzian particles are intrinsically soft (i.e., penetrable), and so the macroscopic reduction parameters of the Rosenfeld scaling (based on kinetic theory concepts for atomistic fluids with strongly repulsive cores) are not appropriate for these systems.

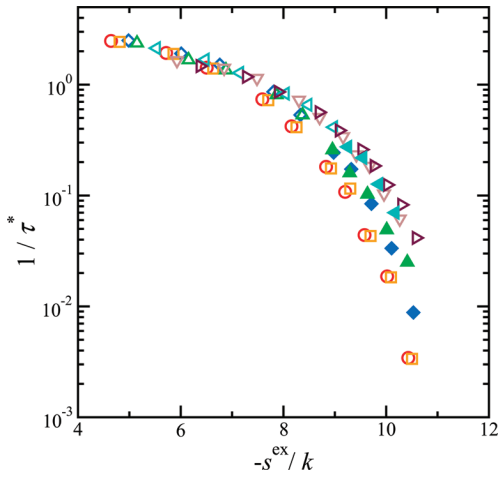

Figure 6. Relationship between the inverse of the reduced collective relaxation time and thermodynamic excess entropy. Symbol notation is the same as for Figure 5.

Interestingly, Krekelberg et al. found that $D_t^*-s_t^{(2)}$ points within the Gaussian-core fluid's anomalous region approximately collapse onto a common curve.[80] Restriction of our $D_t^*-s_t^{(2)}$ data for SPC/E water to points within the anomalous region also reveals a reasonably strong correlation between these two quantities. A similar observation was made by Krekelberg et al. within a study focused on a square-well fluid with short-range attractions.[84] As of yet, the physical rationale for the apparently strong connection between D_t^* and $s_t^{(2)}$ and comparatively weaker connection between D_t^* and s^{ex} within a structurally anomalous region is unclear. Study of several other systems that show anomalous structural and dynamic behavior would be necessary to establish whether this observation is general in that class of fluids.

Figure 6 provides the relationship between the collective relaxation time and the thermodynamic excess entropy. We find a relatively strong correlation between these two quantities when considering all states associated with temperatures above the onset of water's structurally anomalous region. The isochore dependence of $1/\tau^* - s^{ex}$ at low temperature is stronger than what is observed for $D_t^*-s^{ex}$. As one might expect from the discussion above, the correlation between τ^* and $s_t^{(2)}$ is generally poor and is qualitatively similar to the picture presented in the lower panel of Figure 5 for translational diffusivity. The connection between D_t and τ has been examined previously within the context of the Stokes−Einstein (SE) relation. It has been argued[29] that τ serves as a substitute for the viscosity and that the combination $D_t\tau/T$ remains independent of temperature when the SE equation is obeyed. Mazza et al. indicate[29] that there is a breakdown of the SE relation for SPC/E water, with $D_t\tau/T$ increasing sharply at relatively low temperature and low density. From the perspective of Rosenfeld scaling, one expects $D_t^*\tau^*$ data to collapse onto a common curve when plotted versus s^{ex}. Figure 7 contains this relationship. This analysis shows that D_t and τ decouple at relatively low temperature and low density, which is what one expects to find based upon previous reports. The use of entropy scaling concepts to predict $1/\tau^*$ from D_t^* data leads to an overestimate of $1/\tau^*$ at conditions for which the two properties decouple. In other words, straightforward entropy scaling does not capture the enhanced decrease in $1/\tau^*$ relative to D_t^* upon isochoric cooling.

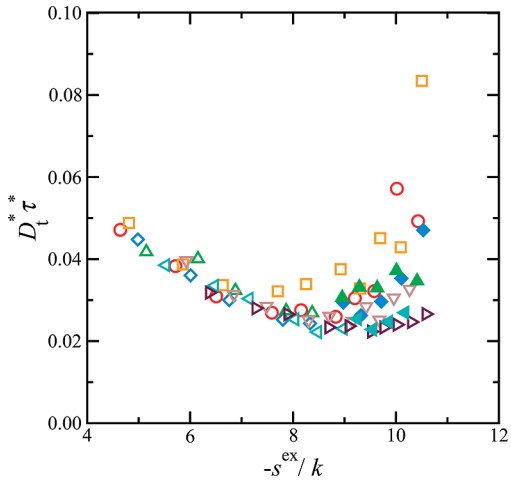

Figure 7. Product of reduced translational diffusivity and reduced collective relaxation time as a function of the thermodynamic excess entropy. Symbol notation is the same as for Figure 5.

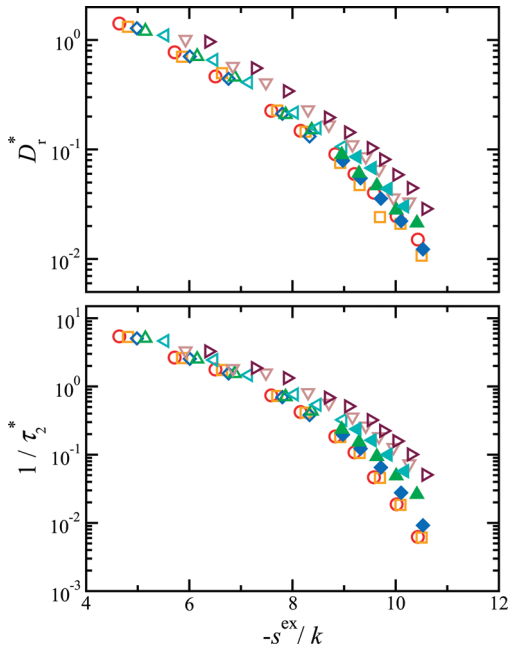

Figure 8. Relationship between reduced rotational diffusivity and thermodynamic excess entropy (top panel) and inverse of the reduced rotational relaxation time and thermodynamic excess entropy (bottom panel). Symbol notation is the same as for Figure 5.

Figure 8 provides the relationships between the two measures of rotational mobility studied here and the thermodynamic excess entropy. For this analysis, D_r^* and $1/\tau_2^*$ provide a consistent description of the connection between rotational mobility and excess entropy. Data collapse is not nearly as good as what is observed for the translational diffusivity and collective relaxation time. While a relatively broad common curve does emerge, one clearly observes isochore dependence to $D_r^*-s^{ex}$ at all temperatures. One can appreciate the difference in the success of Rosenfeld scaling with respect to translational and rotational motion by considering the known decoupling between these two types of motion. A detailed discussion of this issue is included in the recent paper of Mazza et al.[29] Consideration of the Stokes−Einstein and Stokes−Einstein−Debye relations reveals that D_r^*/D_t^* will remain independent of temperature if translational and rotational motions are perfectly coupled. Figure 9a shows the temperature dependence of D_r^*/D_t^* along several isochores. The data indicate that translational and rotational

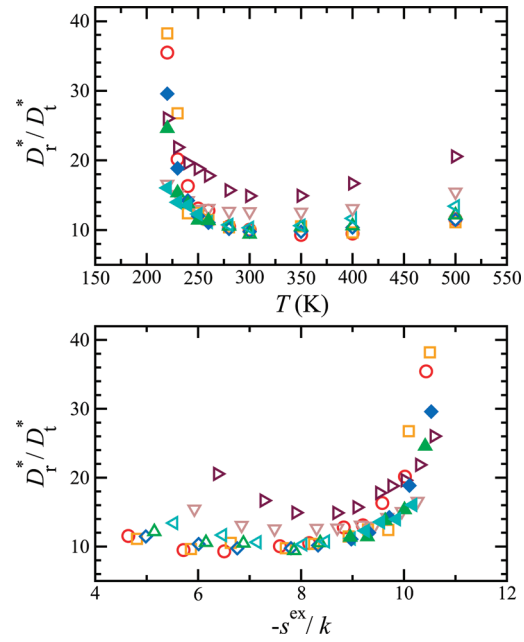

Figure 9. Ratio of the reduced rotational and translational diffusivities expressed as a function of the temperature (top panel) and thermodynamic excess entropy (bottom panel). Symbol notation is the same as for Figure 5.

motion decouple over a wide range of conditions, with the decoupling particularly noticeable at low temperatures. For Rosenfeld scaling to capture translational and rotational mobility equally well, D_r^*/D_t^* would need to collapse onto a common curve when plotted against s^{ex}. It is clear from Figure 9b that this is not the case. This work shows that the thermodynamic excess entropy correlates stronger with translational mobility than rotational mobility.

IV. Conclusions

We have used molecular simulation to investigate connections between dynamic properties and the excess entropy for SPC/E water. Molecular dynamics simulation was used to obtain translational and rotational diffusion coefficients, a relaxation time associated with rotational motion, and a relaxation time intended to probe the collective dynamics of the system. Free-energy-based Monte Carlo simulation methods were used to compute the thermodynamic excess entropy. Our calculations were completed over a wide range of state conditions that included the supercooled liquid regime.

Overall, our analysis suggests that the thermodynamic excess entropy is capable of describing the dynamic properties of a "normal" molecular fluid. At temperatures above the structurally anomalous region of SPC/E water, reduced kinetic property data collapse onto common curves when expressed as a function of the thermodynamic excess entropy. We find that this collapse is particularly good for the translational diffusivity and collective relaxation time and decidedly weaker for the measures of rotational mobility. Within the structurally anomalous region of SPC/E water, X^*-s^{ex} curves, where X^* is a general kinetic property, show isochore dependence. This finding is consistent with previous studies focused on core-softened models that exhibit anomalous behavior. Development of a general formalism for quantitatively relating kinetic and thermodynamic properties of fluids that exhibit anomalous behavior remains an open area of research.

Recent studies suggest that Rosenfeld scaling provides a useful means to describe the transport properties of molecular

fluids. Molecular fluids appear to distinguish themselves from atomistic fluids with regard to the shape of $\ln X^* - s^{ex}$ curves. More specifically, these curves tend to exhibit a more appreciable departure from linear behavior than is observed with atomistic fluids. This departure is particularly noticeable in the case of water. This feature may simply be due to the notion that one can generally probe molecular systems over a broader range of conditions (e.g., supercooled regimes) than is possible with atomistic systems. In any case, it would be of interest to understand how the shape of $\ln X^* - s^{ex}$ curves is linked to the underlying microscopic interactions.

Acknowledgment. J. R. E. acknowledges financial support of the National Science Foundation, Grant No. CBET-0828979. T. M. T. acknowledges support from the Welch Foundation Grant No. F-1696 and from the David and Lucile Packard Foundation. Computational resources were provided in part by the University at Buffalo Center for Computational Research and the Rensselaer Polytechnic Institute Computational Center for Nanotechnology Innovations.

References and Notes

(1) Liu, J.; Lee, J. Y.; Pan, L.; Obermyer, R. T.; Simizu, S.; Zande, B.; Li, J.; Sankar, S. G.; Johnson, J. K. *J. Phys. Chem. C* **2008**, *112*, 2911.
(2) Rosenfeld, Y. *Phys. Rev. A* **1977**, *15*, 2545.
(3) Rosenfeld, Y. *Chem. Phys. Lett.* **1977**, *48*, 467.
(4) Grover, R.; Hoover, W. G.; Moran, B. *J. Chem. Phys.* **1985**, *83*, 1255.
(5) Rosenfeld, Y. *J. Phys.: Condens. Matter* **1999**, *11*, 5415.
(6) Dzugutov, M. *Nature* **1996**, *381*, 137.
(7) Errington, J. R.; Truskett, T. M.; Mittal, J. *J. Chem. Phys.* **2006**, *125*, 244502.
(8) Mittal, J.; Errington, J. R.; Truskett, T. M. *Phys. Rev. Lett.* **2006**, *96*, 177804.
(9) Mittal, J.; Errington, J. R.; Truskett, T. M. *J. Chem. Phys.* **2007**, *126*, 244708.
(10) Mittal, J.; Errington, J. R.; Truskett, T. M. *J. Phys. Chem. B* **2007**, *111*, 10054.
(11) Mittal, J.; Shen, V. K.; Errington, J. R.; Truskett, T. M. *J. Chem. Phys.* **2007**, *127*, 154513.
(12) Goel, G.; Krekelberg, W. P.; Errington, J. R.; Truskett, T. M. *Phys. Rev. Lett.* **2008**, *100*, 106001.
(13) Mittal, J.; Truskett, T. M.; Errington, J. R.; Hummer, G. *Phys. Rev. Lett.* **2008**, *100*, 145901.
(14) Goel, G.; Krekelberg, W. P.; Pond, M. J.; Mittal, J.; Shen, V. K.; Errington, J. R.; Truskett, T. M. *J. Stat. Mech.* **2009**, P04006.
(15) Lazaridis, T.; Karplus, M. *J. Chem. Phys.* **1996**, *105*, 4294.
(16) Mittal, J.; Errington, J. R.; Truskett, T. M. *J. Phys. Chem. B* **2006**, *110*, 18147.
(17) Johnson, M. E.; Head-Gordon, T. *J. Chem. Phys.* **2009**, *130*, 214510.
(18) Abramson, E. H. *Phys. Rev. E* **2007**, *76*, 051203.
(19) Abramson, E. H.; West-Foyle, H. *Phys. Rev. E* **2008**, *77*, 041202.
(20) Goel, T.; Patra, C. N.; Mukherjee, T.; Chakravarty, C. *J. Chem. Phys.* **2008**, *129*, 164904.
(21) Jackson, G.; Chapman, W. G.; Gubbins, K. E. *Mol. Phys.* **1988**, *65*, 1.
(22) Chapman, W. G.; Gubbins, K. E.; Jackson, G.; Radosz, M. *Ind. Eng. Chem. Res.* **1990**, *29*, 1709.
(23) Gerek, Z. N.; Elliott, J. R. *Ind. Eng. Chem. Res.* **2010**, *49*, 3411.
(24) Agarwal, M.; Singh, M.; Sharma, R.; Alam, M. P.; Chakravarty, C. *J. Phys. Chem. B* **2010**, *114*, 6995.
(25) Agarwal, M.; Chakravarty, C. *Phys. Rev. E* **2009**, *79*, 030202.
(26) Agarwal, M.; Ganguly, A.; Chakravarty, C. *J. Phys. Chem. B* **2009**, *113*, 15284.
(27) Mittal, J.; Errington, J. R.; Truskett, T. M. *J. Chem. Phys.* **2010**, *132*, 169904.
(28) Berendsen, H. J. C.; Grigera, R. J.; Stroatsma, T. P. *J. Phys. Chem.* **1987**, *91*, 6269.
(29) Mazza, M. G.; Giovambattista, N.; Stanley, H. E.; Starr, F. W. *Phys. Rev. E* **2007**, *76*, 031203.
(30) Becker, S. R.; Poole, P. H.; Starr, F. W. *Phys. Rev. Lett.* **2006**, *97*, 055901.
(31) Einstein, A. *Investigations on the Theory of the Brownian Motion*; Dover: New York, 1956.
(32) Debye, P. *Polar Molecules*; Dover: New York, 1929.
(33) Nettleton, R. E.; Green, M. S. *J. Chem. Phys.* **1958**, *29*, 1365.
(34) Green, H. S. *The Molecular Theory of Fluids*; North-Holland: Amsterdam, 1952.
(35) Baranyai, A.; Evans, D. J. *Phys. Rev. A* **1989**, *40*, 3817.
(36) Zielkiewicz, J. *J. Chem. Phys.* **2005**, *123*, 104501.
(37) Zielkiewicz, J. *J. Chem. Phys.* **2006**, *124*, 109901.
(38) Zielkiewicz, J. *J. Phys. Chem. B* **2008**, *112*, 7810.
(39) Giuffre, E.; Prestipino, S.; Saija, F.; Saitta, A. M.; Giaquinta, P. V. *J. Chem. Theory Comput.* **2010**, *6*, 625.
(40) Saija, F.; Saitta, A. M.; Giaquinta, P. V. *J. Chem. Phys.* **2003**, *119*, 3587.
(41) Sharma, R.; Agarwal, M.; Chakravarty, C. *Mol. Phys.* **2008**, *106*, 1925.
(42) Errington, J. R. *J. Chem. Phys.* **2003**, *118*, 9915.
(43) Errington, J. R. *Phys. Rev. E* **2003**, *67*, 012102.
(44) Lyubartsev, A. P.; Martsinovskii, A. A.; Shevkunov, S. V.; Vorontsov-Velyaminov, P. N. *J. Chem. Phys.* **1992**, *96*, 1776.
(45) Berg, B. A.; Neuhaus, T. *Phys. Rev. Lett.* **1992**, *68*, 9.
(46) Grzelak, E. M.; Errington, J. R. *Langmuir*, submitted.
(47) Smith, G. R.; Bruce, A. D. *J. Phys. A* **1995**, *28*, 6623.
(48) Fitzgerald, M.; Picard, R. R.; Silver, R. N. *J. Stat. Phys.* **2000**, *98*, 321.
(49) Cichowski, E. C.; Schmidt, T. R.; Errington, J. R. *Fluid Phase Equilib.* **2005**, *236*, 58.
(50) Singh, J. K.; Errington, J. R. *J. Phys. Chem. B* **2006**, *110*, 1369.
(51) Errington, J. R.; Kofke, D. A. *J. Chem. Phys.* **2007**, *127*, 174709.
(52) Kofke, D. A.; Cummings, P. T. *Mol. Phys.* **1997**, *92*, 973.
(53) Kofke, D. A.; Cummings, P. T. *Fluid Phase Equilib.* **1998**, *150*, 41.
(54) Frenkel, D.; Smit, B. *Understanding Molecular Simulation*, 2nd ed.; Academic: San Diego, 2002.
(55) Fenwick, M. K.; Escobedo, F. A. *J. Chem. Phys.* **2004**, *120*, 3066.
(56) Bennett, C. H. *J. Comput. Phys.* **1976**, *22*, 245.
(57) Lu, N. D.; Singh, J. K.; Kofke, D. A. *J. Chem. Phys.* **2003**, *118*, 2977.
(58) Kofke, D. A. *Mol. Phys.* **2004**, *102*, 405.
(59) Shirts, M. R.; Pande, V. S. *J. Chem. Phys.* **2005**, *122*, 144107.
(60) Kammerer, S.; Kob, W.; Schilling, R. *Phys. Rev. E* **1997**, *56*, 5450.
(61) Mazza, M. G.; Giovambattista, N.; Starr, F. W.; Stanley, H. E. *Phys. Rev. Lett.* **2006**, *96*, 057803.
(62) Nosé, S. *Mol. Phys.* **1984**, *52*, 255.
(63) Hoover, W. G. *Phys. Rev. A* **1985**, *31*, 1695.
(64) Swope, W. C.; Andersen, H. C.; Berens, P. H.; Wilson, K. R. *J. Chem. Phys.* **1982**, *76*, 637.
(65) Allen, M. P.; Tildesley, D. J. *Computer Simulations of Liquids*; Oxford University Press: Oxford, 1987.
(66) Martyna, G. J.; Klein, M. L.; Tuckerman, M. E. *J. Chem. Phys.* **1992**, *97*, 2635.
(67) Andersen, H. C. *J. Comput. Phys.* **1983**, *52*, 24.
(68) Truskett, T. M.; Torquato, S.; Debenedetti, P. G. *Phys. Rev. E* **2000**, *62*, 993.
(69) Errington, J. R.; Debenedetti, P. G. *Nature* **2001**, *409*, 318.
(70) Shell, M. S.; Debenedetti, P. G.; Panagiotopoulos, A. Z. *Phys. Rev. E* **2002**, *66*, 011202.
(71) Sharma, R.; Chakraborty, S. N.; Chakravarty, C. *J. Chem. Phys.* **2006**, *125*, 204501.
(72) Agarwal, M.; Chakravarty, C. *J. Phys. Chem. B* **2007**, *111*, 13294.
(73) Harrington, S.; Poole, P. H.; Sciortino, F.; Stanley, H. E. *J. Chem. Phys.* **1997**, *107*, 7443.
(74) Lynden-Bell, R. M.; Debenedetti, P. G. *J. Phys. Chem. B* **2005**, *109*, 6527.
(75) Agarwal, M.; Sharma, R.; Chakravarty, C. *J. Chem. Phys.* **2007**, *127*, 164502.
(76) Yan, Z.; Buldyrev, S. V.; Giovambattista, N.; Stanley, H. E. *Phys. Rev. Lett.* **2005**, *95*, 130604.
(77) Yan, Z.; Buldyrev, S. V.; Giovambattista, N.; Debenedetti, P. G.; Stanley, H. E. *Phys. Rev. E* **2006**, *73*, 051204.
(78) Krekelberg, W. P.; Mittal, J.; Ganesan, V.; Truskett, T. M. *Phys. Rev. E* **2008**, *77*, 041201.
(79) Starr, F. W.; Sciortino, F.; Stanley, H. E. *Phys. Rev. E* **1999**, *60*, 6757.
(80) Krekelberg, W. P.; Kumar, T.; Mittal, J.; Errington, J. R.; Truskett, T. M. *Phys. Rev. E* **2009**, *79*, 031203.
(81) Pond, M. J.; Krekelberg, W. P.; Shen, V. K.; Errington, J. R.; Truskett, T. M. *J. Chem. Phys.* **2009**, *131*, 161101.
(82) Krekelberg, W. P.; Pond, M. J.; Goel, G.; Shen, V. K.; Errington, J. R.; Truskett, T. M. *Phys. Rev. E* **2009**, *80*, 061205.
(83) Fomin, Yu. D.; Ryzhov, V. N.; Gribova, N. V. *Phys. Rev. E* **2010**, *81*, 061201.
(84) Krekelberg, W. P.; Mittal, J.; Ganesan, V.; Truskett, T. M. *J. Chem. Phys.* **2007**, *127*, 044502.

JP1049155